

Families In Wild Multimedia (FIW-MM): A Multi-Modal Database for Recognizing Kinship

Joseph P Robinson, *Student Member, IEEE*, Zaid Khan, *Student Member, IEEE*, Yu Yin, *Student Member, IEEE*, Ming Shao, *Member, IEEE*, Yun Fu *Fellow, IEEE*

Abstract—Kinship is a soft biometric detectable in media with an abundance of practical applications. Despite the difficulty of detecting kinship, annual data challenges using still images have consistently resulted in improved performances and attracted new researchers. Now, systems are reaching performance levels unforeseeable a decade ago, closing in on performances acceptable for real-world use. Similar to other biometric tasks, we expect that systems can benefit from additional modalities. We hypothesize that adding modalities to FIW, which contains only still images, will improve performance. Thus, to narrow the gap between research-and-reality and enhance the power of kinship recognition systems, we extend FIW with multimedia (MM) data (*i.e.*, video, audio, and text captions). Specifically, we introduce the first publicly available multi-task MM kinship dataset. To build FIW-MM, machinery was developed to collect, annotate, and prepare the data automatically, requiring minimal human input and no financial cost. The proposed MM corpus allows us to formulate problems following more realistic template-based protocols. We show significant improvements in all benchmarks with the added modalities. The results are analyzed by highlighting edge cases to inspire future research with different areas of improvement. FIW-MM provides the data required to increase the potential of systems built to automatically detect kinship in MM. It also allows experts from diverse fields to collaborate in new ways.

Index Terms—Kinship Verification, Visual Information, Audio, Multi-Modal Data, Feature Fusion, Deep Learning, Template Adaptation.

1 INTRODUCTION

AUTOMATED kinship recognition assumes genetic relatedness between individuals is detectable by facial cues - a task unimaginable a decade ago. Progress in this difficult task has been driven largely by kinship datasets and concurrent advances in face recognition (FR) [1], [2]. The seminal work in visual kinship recognition introduced the first image dataset in 2010 [3], which was later followed by larger and more difficult datasets, such as *Families In the Wild* (FIW) [4] and *Tri-Subject Kinship* (TSKIN) [5]. In response, vision researchers developed methods and models to match the rising level of difficulty in kinship datasets [6], [7].

Conventional FR systems are capable of acquiring, storing, and recognizing human faces automatically. Nowadays, FR technology and the different sub-problems that model visual knowledge from facial cues have grown popular in speaker-based problems based on audiovisual data (*e.g.*, speaker separation [8], speaker identification [9], [10], cross-modal audio-to-visual or vice-versa [11], emotion recognition in multimedia (MM) [12], [13], and several others [14], [15]). The sudden surge of attention to audiovisual data has brought together experts who specialize in biometric signals to share thoughts, combine knowledge, and propose solutions that best fuse multi-domain knowledge for optimal decision making [16], [17]. The benefits of added biometrics signals reaped in FR, intuitively, can also enhance existing state-of-the-art (SOTA) in kinship recognition.

However, acquiring paired data of multiple modalities is challenging.

For this, we start with the aforementioned FIW image collection [4], [18]. It has family tree structures for 1,000 disjoint families, each with ≥ 12 family and profile photos of many members (*i.e.*, averaging 20 faces for $5 \geq$ members ≥ 22). Metadata includes surnames, first names, gender, bounding box coordinates for instances of each the respective member appearing in a photo, along with the connections (or lack thereof) with all the other members of that family. To extend FIW with the multimedia data needed to test our hypothesis, we chose 200 families of FIW such that ≥ 2 members will then have video data as well (*i.e.*, video tracks, audio, and contextual data as biometrics concerned with modalities in addition to appearance from imagery like visual dynamics from video, speech (sound) from audio, and spoken words from text captions).

This work shows that the addition of MM for kin-based recognition can improve the current SOTA. Specifically, our contributions to the FR, biometric, anthropology, and MM communities can be summarized in three-fold.

- **Built multimedia database:** an extension of the large-scale FIW image set with MM data (*i.e.*, video tracks, audio segments, visual-audio clips, and text transcripts) acquired with an automatic labeling scheme— >600 video and speech samples for 2 or more members of 200 FIW families). The MM family database was restructured to better encapsulate the added meta-data and paired data respectively at the subject and instance levels.
- **Recorded protocols and benchmarks:** a new paradigm for kinship recognition made possible with the MM data. Specifically, the experiments are

• J.P. Robinson, Y. Yin, Z. Khan, and Y. Fu was with the Department of Electrical and Computer Engineering, Northeastern University, Boston, MA, 02115. E-mail: see <http://www.jrobsvision.com>

• M. Shao was with University of Massachusetts, Dartmouth, MA, 02747.

Manuscript received October 1, 2020; revised XXX ##, 202?.



Figure 1: Sample family of FIW in Multimedia (FIW-MM). Top-to-bottom: *family-tree labels* show faces of members in the immediate family, with subjects of the same generations in the same row; *videos, audio, and contextual* exemplify sample video pairs of Dr. King Jr. and his daughter Andrea with tracklets of faces in the visual domain and audio data aligned frame-by-frame; *family photos* that contain Dr. Luther King Jr. randomly selected (note, cropped to fit); *faces* of Dr. King Jr. from adolescence-to-adulthood. Multiple faces are available for most subjects. Best viewed electronically.

template-based, opposed to instance-based, for there are often variable number of samples per subject in real-world settings. Thus, we are the first to measure kinship recognition capabilities using a multimodal template-based collection with family tree labels .

- Showed the advantage of all modalities: Following the improved protocols and, thus, experimental settings, we demonstrate an increase in system performance from still-images, to still-images and videos, and then with audio speech signals added as well– a clear benefit of each added modality is shown. Our analysis highlights the shortcomings of the different media types for future work to address.

We believe this will attract a wider range of scholars to kin-based and multimedia problems. FIW-MM will be accessible online in various formats.¹

1. FIW-MM - the data, code, trained models, and other resources - will be available upon publication of this work.

2 RELATED WORK

Early on, problems of recognizing kinship started with domesticated animals (e.g., dogs [19] and sheep [20], [21]), as many species have a natural ability to recognize their kin through various signals (e.g., touch, smell, visual, and acoustics). From this, we hypothesized that different types of media, besides image-level or conventional speech recognition, can be leveraged to better detect kinship in humans. Knowledge extracted from still-images and stationary speech signals are lacking an abundance of evidence. A more complex signal which helps improve decision making, such as dynamic features across video frames, can attribute inheritable characteristics (e.g., expressions, mannerisms, and accents from different emotions). Nonetheless, such technology will take effort to acquire. We demonstrate the ability of the added modalities with face tracks from videos and standard audio features from speech signals.

We next review existing work in visual kinship recognition on still-images, and then more recent advances in the acquiring and modeling of visual-audio data for FR.

Table 1: Commonly used acronyms and variables.

DB Terms	FID	Family ID
	MID	Member ID
	PID	Picture ID
	VID	Video ID
Pair-types	BB	Brother-brother
	SS	Sister-sister
	SIBS	Brother-sister
	FD	Father-daughter
	FS	Father-son
	MD	Mother-daughter
	MS	Mother-son
	GFGD	Grandfather - granddaughter
	GFGS	Grandfather - grandson
	GMGD	Grandmother - granddaughter
	GMGS	Grandmother - grandson
	GGFGD	Great GFGD
	GGFGS	Great GFGS
	GGMGD	Great GMGD
	GGMGS	Great GMGS
Tri-Pairs	FMD	father/mother-daughter
	FMS	father/mother-son
Metrics	CMC	Cumulative matching characteristic
	DET	Detection error trade-off
	FAR	False-acceptance rate
	ROC	Receiver operating characteristic
	TAR	True-acceptance rate
Task / solution	FR	Facial recognition
	SVM	Support vector machine
	TA	Template Adaptation
Experimental	P	Probe
	G	Search gallery
	X	Template
	x	Media sample
	x^+	Encoded media sample
	x^-	No. positive templates
	z	Encoded media sample
	N_+	No. positive templates
	N_-	No. negative templates

2.1 Kinship recognition

Computer vision researchers began using facial cues to recognize kinship about a decade ago. Specifically, Feng *et al.* proposed to model the geometry, color, and low-level visual descriptors extracted from faces to discriminate between KIN and NON-KIN [3]. Others then formulated the problem as various paradigms (*e.g.*, transfer subspace learning [22], [23], 3D face modeling [24], low-level feature descriptions [25], sparse encoding [26], metric learning [27], tri-subject verification [5], adversarial learning [28], ensemble learning [29], video understanding [30]–[32], and, most recently, video-audio understanding [33]). A common factor of the aforementioned was the attempt to improve discriminatory power for classifying a pair of faces as either KIN or NON-KIN; another commonality was the limited sample size and, thus, unrealistic experimental settings.

Robinson *et al.* introduced a large-scale image dataset to recognize families in still-imagery called FIW [18], [34]. FIW contains 1,000 families with an average of 13 family photos, 5 family members, and 26 faces. It came with benchmarks for 11 pairwise types, with the top performance of the baselines being a fine-tuned CNNs (*i.e.*, SphereFace [1] and Center-loss [35]). This was the beginning of big data in kin-based vision tasks— deep learning could then be used to overcome observed failure cases [36], [37]. Furthermore, new applications such as child appearance prediction [38], [39] and familial privacy protection [40] were done recently.

Nowadays, FIW continues to challenge researchers with various views of image-based tasks. A myriad of methods demonstrated the ability of machinery to use still-images to determine kinship in a pair or group of subjects. Nonetheless, only so much information can be extracted from still-images. The dynamics of faces in video data (*e.g.*, mannerisms expressed across frames) contain additional information, and audio as well as text transcripts (*i.e.*, contextual data describing the speech and other sounds) can widen the range of cues we model to discriminate between relatives and non-relatives. We propose the first large-scale multimedia dataset for kinship recognition. Specifically, we leveraged the familial data of the FIW image database to build upon the existing resource [18], [34], using the still-images of FIW and adding video, audio, audiovisual, and text data of subjects. Note that the difference between the video and audio compared to the visual-audio is that the former two are single modality and the latter has multiple modalities—visual-audio clips contain a talking face tracks aligned with the speech signal. After its predecessor, database was dubbed FIW-MM. En route to bridging research-and-reality, we follow the protocols of FIW [7], but now with the capacity to be template-based (*i.e.*, per National Institute of Standards and Technology (NIST) in [41]). Figure 1 depicts a sample family with MM for MLK and his daughter.

Besides the different use-cases, and independent research work it made possible, FIW was used as part of an annual data challenge motivated to attract more attention from and provide more incentive for the research community. Namely, the *Recognizing Families In the Wild* (RFIW) data challenge series, which has been held annually since 2017 [42], and with the latest in 2020 [43]. There have been many great attempts on the still-images as a result [44], [45]. Recent surveys [46], tutorials [4], and challenge papers [7], [47]–[49] elaborate on RFIW and the various submissions in detail.

2.2 Audio-visual data

The archetypal big data resources for audio-visual identification problems are Voxceleb [9] and Voxceleb2 [10]. Similar to FIW-MM, the datasets were acquired by extending still-image collections (*i.e.*, Voxceleb and Voxceleb2 extended of the VGGFace [50] and VGGFace2 [51], respectively). Currently, the primary usage of Voxceleb is in speaker-based tasks, such as using the audio-visual data to detect and classify the speaker by the *who* and the *when* [8]. Additional speaker centric problems have been proposed using the Voxceleb collections, like to enhance speech signals [52], to detect *when* and *where* the speaking face is visible [53], and when the audio and mouth motions infer the lips and sound are in sync [54]. Nonetheless, the lip-reading task predates the larger Voxceleb with older lip-reading datasets [55], [56].

It is worth highlighting that these audio-visual databases were instrumental in applied research as well (*e.g.*, generating talking faces [57], where the input is a still-image face and a stream of audio, and the output are frames mocking the audio with the faces as if the input face was regurgitating the audio clip). In [58], face frames were generated from a still image and audio clip, with pose information added as a control signal for the synthesized output. Furthermore,

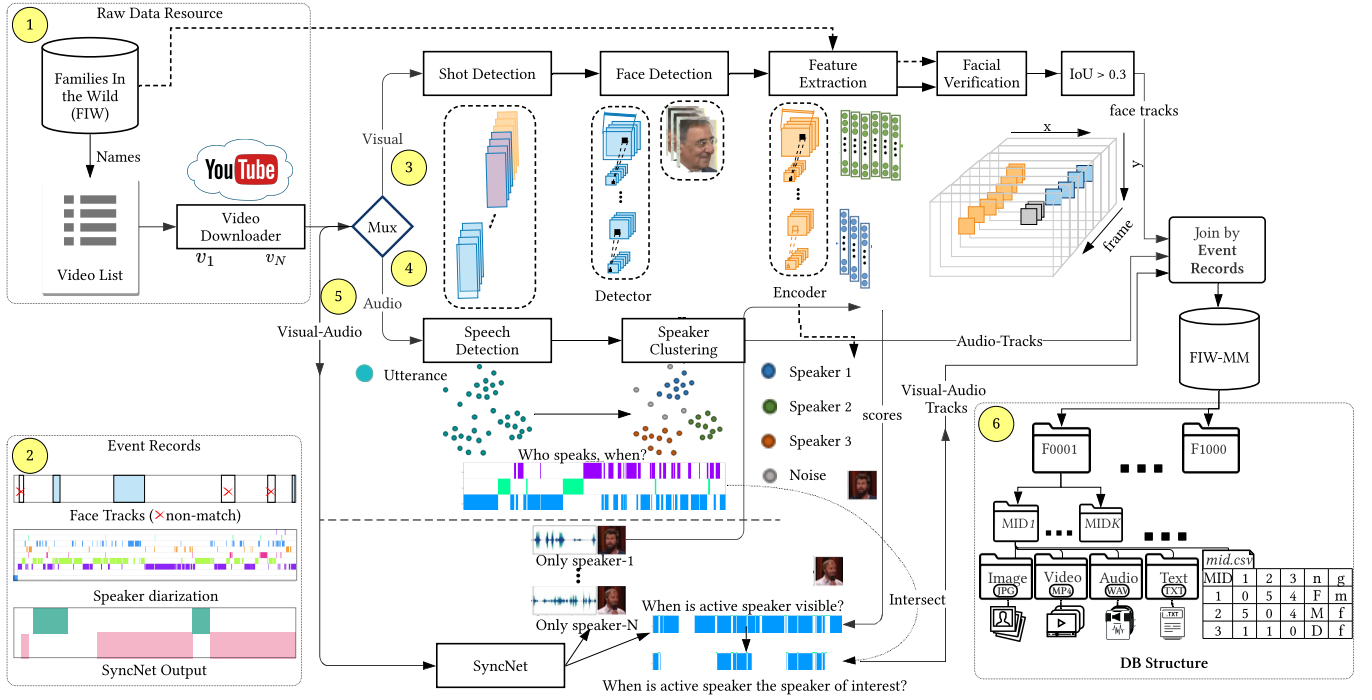


Figure 2: Automated labeling framework. (1) A single family was extended with N YouTube videos. Next, a single video was processed per iteration: (2) instantiate three event records with t indices to match the frame count of video v_i (i.e., $i \in \{1, N\}$) for which events of branch 3-5 get recorded. (3) Process visual data by detecting faces tracks per video shot and recording as event if a *match* compared with FIW. (4) Transform audio to speech utterances, cluster speaker IDs as k clusters for k subjects, and record as events. (5) Use audio-visual data to determine the frames showing the active speaker to then record as events. The event records were compared to filter the samples of interest via logic before (6) storing MM data in FIW-MM database. Details for each step are provided in Section 3.2.

Voxceleb predicted emotion labels via its own signals to automatically infer ground-truth [59].

Previous attempts to tackle kinship recognition have also been made with audio-visual data. Most relevant was in [33], where the authors built a collection made-up of 400 pairs. Wu *et al.* certainly demonstrated the core hypothesis of this work—multimedia can enhance our ability to automatically detect kinship in humans—as was clearly demonstrated in their work [33]. However, the sample size was limited in the number of pairs and in the types of labels, as there is no family tree structure, nor multiple samples per member (i.e., age-varying), as is the case in our much larger and comprehensive FIW-MM.

3 THE FIW-MM DATABASE

FIW-MM used existing paired face data of FIW² as a part of an automated labeling pipeline that allowed it to be acquired with no financial cost and minimal human input (Figure 2). Specifically, the labeled FIW allowed us to identify *who*, *when*, and *where* a family member appeared in the video. We chose a subset of 200 (of 1,000) FIW families for which 2-5 members are in 1-3 YouTube videos: a total of 550 subjects in 660 videos. Three types of data were collected per subject per video: non-speaking face tracks (visual only), speech segments (audio only), and face tracks of speaker

(visual-audio). Time-stamps are set for the start and end frames, along with the bounding box information for the face tracks. In this way overlap in samples were identifiable.

Let us next cover the data specifications, along with a detailed description of our automatic labeling pipeline.

3.1 Specifications

The goal was to extend FIW in the number of samples and the types of media. Plus, improved experimental protocols. Recalling that FIW provides name metadata and face images for multiple members of 1,000 families [4], we were able to use this from the 200 families. For quick reference, common acronyms and symbols are listed in Table 1.

Following convention of the original FIW [18], the indices of the topmost level of the database were unique Family IDs (FIDs), which contain M Member IDs (MIDs) for M family members. Each FID is represented by a relationship matrix of size M (i.e., a row and a column added per MIDs), along with the gender information for each member. Thus, FIW is organized with 1,000 folders (i.e., one per FID, F0001-F1000), each with a relationship matrix that relates the M MIDs that have face data stored in subfolders (e.g., family F0009 has $M = 7$ meaning the folder contains 7 MID folders, MID1, ..., MID7). The same scheme is adopted for FIW-MM, with the difference being that the MID folders now contain a folder per media type (i.e., subdirectory *images* added to MID folder for which existing face images are now stored).

2. <https://web.northeastern.edu/smilelab/fiw/download.html>

Table 2: Database statistics. Types are split based on the span in generation of the relationship.

m	1^{st} -generation			2^{nd} -generation				3^{rd} -generation				4^{th} -generation				Total
	BB	SS	SBS	FD	FS	MD	MS	GFGD	GFGS	GMGD	GGMGS	GGFGD	GGFGS	GGMGD	GGMGS	
# Subjects	883	824	1,542	1,914	1,954	1,892	2,041	426	463	483	526	39	30	45	37	13,099
# Families	345	334	472	666	676	665	670	154	174	178	191	9	10	11	10	953
# still-images	40,386	31,315	46,188	83,157	89,157	57,494	63,116	8,007	6,775	6,373	6,686	408	410	798	797	441,067
# Clips	123	79	81	155	134	147	138	16	18	25	15	2	4	0	0	937
# Pairs	641	621	1,138	1,151	1,253	1,177	1,207	263	280	292	324	28	18	36	28	8,457

Besides, additional folders for different media types were added for subjects extended with MM data.

3.2 Data pipeline

Inspired by previous work, such as FIW [34] (*i.e.*, labeling families) and VoxCeleb [9] (*i.e.*, labeling audio-visual data), we formed the basis for our pipeline. From this, three modality-specific branches processed the data independently. Specifically, the branches process the *video*, *audio*, and *audio-visual* modalities. Furthermore, branch-specific events are recorded by the frame number and used to summarize particular instances that are propagated between records.

The following subsections are numbered according to the yellow circle call-outs in Figure 2.

Step 1. Raw data resource. A single family with at least two members on Youtube was selected (*i.e.*, families with only one member with MM would be useless). Video URLs were queried per unique Video IDs (VIDs) (*i.e.*, v_1, \dots, v_N for N videos). Generally speaking, the videos were either interview-style (*e.g.*, with only a news anchor in a plain room answering scripted questions) or face-time clips (*i.e.*, self-recordings with the subject speaking directly to the camera). Also, the ethnicity for subjects were manually collected.

We used Pypi’s youtube-dl³ to download YouTube videos by URL: each renamed as its VID and stored as MKV file, along with TXT with captions when available. The raw data consists of the original MKV for the *audio-visual* branch, along with audio only (WAV) and visual only (MP4) extracted with *ffmpeg* assuming 25 FPS.

Step 2. Event records. Before branching, blank (sequential) tabular records were instantiated for the duration of the video— one record per branches denoted 3-5 (*i.e.*, audio, visual, and audio-visual event records). These are later compared to share knowledge between the branches to help filter out samples of the subject of interest. In essence, the mutual information across records at a given instance (*i.e.*, frame-step) are used to imply matches, contradictions, and non-matches across modalities (*i.e.*, a means to propagate labels across modalities). The usage of set theory helps to both validate *matches* and filter out *non-matches*. Although unique to our problem, the concept of using logic across events to parse videos has been done (*e.g.*, [60]); however, opposed to high-level semantics like types of objects, we care about the simpler tasks of face or no face, speech or non-speech, visible or unseen, and then the same or different subject. Furthermore, doing this increases the random chance by adding additional evidence across-records.

Specifically, and for one video at a time, the three event records are instantiated with zero event entries. Then, events of each branch are recorded. The type of event are later described for each branch: like branch 3, visual branch, the

events are face tracks that is are a *match* with BB coordinates recorded for all frames of the shot; the audio branch consists of instances that each of the k speakers pronounce utterances; the record for the audio-visual branch are when the speaker is visible in the current frame. Then, by propagating knowledge of frame number that the subject of interest appears, the other audio instances with the same speaker and the frames where the speaker are visible can be inferred by finding intersecting events between the three records.

Step 3. Visual branch. A video was first parsed into scenes by using two global measures and with the assumption that, statistically, neighboring frames of the same shot will match as close as 90% when comparing HSV (*i.e.*, color) and local binary patterns [61] (*i.e.*, texture) features. The aforementioned features were extracted and used to parameterize two probabilistic representations per frame (*i.e.*, one per feature). Then, neighboring frames were measured via KL-Divergence and compared with a threshold of 0.1 [62]. A pair of frames that scored below the threshold were assumed to be shot boundary frames for V videos of size T , *i.e.*, $v_t \in \{1, \dots, C\}$ represents all shots detected in the i -th video. The first, last and the frame closest to the centroid (*i.e.*, in color and texture) were used to represent the shot: the three frames were run through a MTCNN face detector [63], and for those without at least one face detection were assumed face-less scenes. Otherwise, the clips with face detections had as many as five additional frames sampled and passed to the face detector, and then all faces were encoded and compared to the faces for members of the respective family in FIW. Events were then recorded for the face tracks that were a *match* with the subject of interest. Note that this was a means to quickly drop unwanted data, and reduce noise in events assumed by the other branches.

Faces were encoded with ArcFace via the architecture, settings, and *matcher* of [64]. Specifically,

$$d_{bool}(x_i, x_j) = d(x_i, x_j) \leq \theta, \quad (1)$$

where the *matcher* $d_{boolean}$ compared the i -th face detected to j -th FIW face encoding [65]. Hence, $d_{boolean}$ is the decision boundary in score space— if threshold θ is satisfied, assume *match*; else, *non-match*. Note that it is currently assumed that i and j are from different sets (*i.e.*, with J labeled samples from FIW and I face detections from newly collected). The *matcher* in Eq 1 was set as cosine similarity the closeness of the L2 normalized [66] encodings by $d_{bool}(x_i, x_j) = 1 - d(x_i, x_j) = \frac{z_i \cdot z_j}{\|z_i\|_2 \|z_j\|_2} > \theta$, where z represents media encoding. We set $\theta = 0.2$ manually for a high recall. This process - including the usage of ArcFace to encode faces - is the *matcher* used throughout.

In the end, scenes containing the subject of interest had all its frames processed by the MTCNN— the bounding box

3. <https://github.com/ytdl-org/youtube-dl/>

Table 3: Task-specific counts: Individuals (I), families (F), still-face images (S), video-clips (V), audio snippets (A), audio snippets (VA) in the set of probes (P), gallery (G), and in total (T).

		Train					Val					Test				
		I	F	S	V	A	I	F	S	V	A	I	F	S	V	A
T1	T	2,976	571	16,464	290	7,217	955	190	5,458	72	3,308	972	192	5,231	91	1,775
	P	571	571	3,039	47	1,843	190	190	1,334	16	789	192	192	993	23	876
T3	G	2,475	571	13,571	244	5,581	791	190	4,538	56	2,519	800	192	4,705	69	899
	T	3,046	571	16,610	291	7,424	981	190	5,872	72	3,308	992	192	5,698	92	1,775

coordinates, fiducials (*i.e.*, 5 points), and confidence scores were recorded for each step. We then processed the BB coordinates to ensure continuity, dropping those without it: the ROI was set on the previous face location, and the IoU was calculated frame-by-frame, which had to surpass a threshold of 0.3. Finally, up to 25 (*i.e.*, J) faces were sampled per track, and passed to d_{bool} with each of the I labeled faces (*i.e.*, producing $J \times I$ score matrix). The mean across I samples produced a single score per the J faces, at which point the value at the 25-percentile was compared to a higher threshold of $\theta = 0.25$. Note, the fusion of scores was done to both consider all the existing labeled faces equally, while avoiding much weight on any of the few (of J) potentially low-quality faces. This step alone yielded many face tracks of type *match* with a high confidence.

Step 4. Audio branch. Audio signals was extracted from the videos and saved as high-quality WAV files. For the entire audio clip we did speaker diarization– the process of detecting utterances of speech (*i.e.*, the *when*), to then form K clusters for K speakers (*i.e.*, the *who*). Note that the clusters are arbitrarily assigned IDs per video. In the end, a speech detector determined the *when*, and clusters determined the number of speakers and, thus, the speech segments from the *who*. The utterance detector used was SpeechRecognizer⁴, and clusters were based on models from [67].

Step 5. Visual-audio branch. Aimed to detect when the speaker is in the field of view. Thus, the purpose was to find the frames for which the face and speech were aligned. An intuitive way would be to relate the faces detected, lip motions, and audio– which is at the core of many speaker ID methods in MM [68]. For this, videos were processed using SyncNet [69]), pre-trained from [70]. The output were the BB at frames for which the audio aligned to that face.

Using the event records of the *visual branch*, the faces tracks belonging to the subject of interest were determined and used to record events as such. Furthermore, these events compared with the audio events allowed the cluster containing all speech utterances of the subject of interest formed at Step 4 to be determined.

Step 6. Outputs and DB structure. The face tracks, audio segments, and audio-visual tracks of the subject of interest are output and retractable via the final event record (*i.e.*, the three records merged with only positive instances). Thus, overlap between audio and visual-audio infers which cluster of audio segments belongs to the respective active speaker, while the processing of the visual and comparison to the original FIW allowed for the subject of interest to match up with the active speaker. Any overlap in the

data found in the *visual branch* or *audio branch* versus the *audio-visual* were removed as duplicated instances. The face tracks, speech segments, and clips with aligned visual-audio were added to the folder named after media type in the MID folders, along with the final event record (*i.e.*, the event record is enough to parse raw data). Then, the database is N FID folders with M MID-folders and a relationship matrix.

4 PROBLEM STATEMENTS

Following the protocols of the recent RFIW data challenge [7], we benchmark two kin-based tasks: kinship verification and search & retrieval of family member. In RFIW, and the contemporary works in kinship recognition, protocols are image-based *i.e.*, uni-modal, *single-shot* experiments. By contrast, FIW-MM supports multi-modal, with additional samples and media types (Table 2). Provided the MM, protocols are template-based, like with IJB-A [41].

Kinship verification has been the primary focus for experiments. More recently, the emergence of the more challenging, but more practical, task of *searching for missing family members* was supported [7]. We benchmark FIW-MM for both tasks. With the difference being the template-based [41]– approaching settings of operational use-cases.

We next provide details for the paradigms for template-based recognition tasks. We then describe the tasks: first kinship verification; then search & retrieval of family members. The paragraph structure is the same for both: task overview, data splits and settings, and task-specific metrics.

4.1 Definitions and protocols

Template X contains all media for a subject (*i.e.*, images, videos, audio-clips). Hence, X consists of samples x , with a total of N templates for the n^{th} independent piece of media x_n , with a size of the sum of all data samples, $N = N_I + N_V + N_A$. Typically, we store a feature encoding per media sample– we know assume templates are containing feature vectors via $\mathcal{F}(x) = z$, where \mathcal{F} maps faces to a feature space by $\mathcal{F}(x) \in \mathbb{R}^d$, where the dimension d is the size of the encoding. Subject-specific templates are set as either probe P (*i.e.*, query) or reference Q (*i.e.*, hypothesis). For 1: N , known subjects are from a known family, templates enroll in gallery G . Then, at inference, the goal is to match an unseen probe P with a G , where $|G|$ refers to number of templates enrolled. As we will discuss, for 1:1, we assume $|G| = 1$ (*i.e.*, compare template of P with the template of G , and determine whether pair is *KIN* or *NON-KIN*). On the other hand, $|G| > 1$ for the one-to-many 1: N search

4. https://github.com/Uberi/speech_recognition

Table 4: True Acceptance Rate (TAR) (%) at specific False Acceptance Rate (FAR). Scores are for template-based settings: still-images only (left column), +videos (middle), and +video+audio (right). Higher is better.

FAR/ TAR	BB			SS			SIBS			FD			FS			MD			MS			Avg.		
0.5	97.8	97.8	98.2	91.5	92.3	92.7	91.7	90.8	91.5	79.8	77.8	79.9	85.3	85.3	87.1	90.6	88.8	91.4	81.3	82.6	85.2	88.3	87.9	89.8
0.3	94.1	94.1	95.3	88.0	87.2	90.1	82.9	83.9	85.7	63.5	66.5	69.3	77.1	79.1	81.5	82.4	82.3	85.0	68.9	70.1	73.4	79.6	80.4	81.6
0.1	88.1	87.4	88.4	76.1	76.1	79.1	68.7	68.2	70.2	34.5	36.9	42.9	54.3	54.3	58.2	62.2	63.1	69.4	46.1	46.5	50.1	61.4	61.8	64.9
0.01	70.4	70.4	73.6	54.7	55.6	59.9	44.2	46.1	52.4	5.9	7.9	12.9	23.6	24.0	32.1	28.3	31.3	40.6	11.6	13.3	21.0	34.1	35.5	41.1
0.001	54.8	57.0	61.1	47.9	48.7	52.4	29.5	29.0	33.7	2.0	2.5	7.7	9.3	10.9	14.1	14.2	14.6	18.5	3.3	4.6	7.8	23.0	23.9	30.1

& retrieval task as the output are ranked lists of template IDs sorted by the likelihood of being a family member (*i.e.*, if $|G| = 10$, then template of P will compare with the 10 templates of G , to generate a list of indices $[1, 10]$ ordered by score when compare with probe P .)

As mentioned, an audio segment (*i.e.*, a clip of subject speaking without interruptions or major pauses) is also treated as a single piece of media x , which is fused to a single representation by averaging across frames. Note that a video may consist of several disjoint tracks visual, audio, and visual-audio (*i.e.*, aligned). Thus, there are many independent media samples for both the visual and audio modalities. Again, this is the set of media a subject's template X assumes, made up of these various media samples x , such that the j^{th} subject can be represented by k media samples as follows: $X_j = \mathcal{F}_t(x_1), \mathcal{F}_t(x_2), \dots, \mathcal{F}_t(x_k)$, where t corresponds to the media type and, hence, the corresponding encoder. From this, $|X_j|$ is the total number of encodings for subject j . The *gallery* G consists of a set of subjects by $G = \{(X_1, y_1)^l, (X_2, y_2)^l, \dots, (X_n, y_n)^l\}$, where y are identity labels for each of the N subjects, and $l \in \{1, 2, \dots, L\}$ are ground-truth for L families. To establish a precise definition for problems of kinship, each tuple also contains a tag representing the set of L families (*i.e.*, $(X_j, y_j)^l$), where $l \in \{1, 2, \dots, L\}$. Further partitioning of the data is done per requirements of a task. For instance, for the verification, the i^{th} pair of tuples from the same family $\mathbb{P}_m = ((X_i, y_i) \cap (X_j, y_j))$, where $i \neq j$, inherit labels KIN (*i.e.*, *match*) and relationship type.

Each task consists of a ($\approx 60\%$) train, ($\approx 20\%$) validation, and ($\approx 20\%$) test set. These sets are disjoint in family and subject IDs—sets were generated by splitting family labels, with partitioning that remained constant for all tasks.

4.2 Kinship verification

Kinship verification is the simpler of tasks in this challenging and complex topic. Hence, this one-to-one paradigm is the main view vision researchers have tackled. The task is to determine whether a face-pair are blood relatives (*i.e.*, *true kin* or *match*). This face-based problem inherits all the challenges of conventional FR such as variations in lighting, pose, and occlusion (*e.g.*, sunglasses or beards). Additionally, several challenges specific to kin-based FR are posed by age variations, face pairs that contradict directional relationships (*e.g.*, grandparent-grandchild, where the face image of the grandfather was from a younger age and that of the grandchild was older), bias in across subgroups like in FR [43] but amplified for the kin-based data.

The most fundamental question asked in kinship verification, and re-asked in all other kinship discrimination tasks, is whether a face pair is related. Therefore,

kinship verification is boolean classification of pairs (*i.e.*, $y \in \{KIN \cup NON-KIN\}$). Typically, knowledge of the relationship type is assumed. Thus, provided the output of the model for a given pair is *KIN*, then the specific type is implied. Future efforts could incorporate relationship-type signals to advance capabilities of kinship detection systems; however, and as stated upfront, verification provides the simplest of all the benchmarks and, up until now, is the most popular [7].

4.2.1 Data splits and settings

Conventionally, a query consists of a single face image x_1 paired with a second face image x_2 (*i.e.*, a one-shot, boolean classification problem with labels $y \in \{KIN, NON-KIN\}$). Put formally, given a set of face-pairs $(x_1, x_2)_s^l$, where the number of sample pairs $s \in \{1, 2, \dots, S\}$ of relationship-type (*e.g.*, *mother-son*). A set of pair-lists $\mathbb{P} = \{[(x_1, x_2)_1^l], [(x_1, x_2)_2^l], \dots, [(x_1, x_2)_S^l]\}$ for the L types, and with the label determined by the indicator function $\mathbb{1}$ for a single pair $\mathbb{P}_s \rightarrow \{0, 1\}$, *i.e.*,

$$\mathbb{1}(\mathbb{P}_s) = \begin{cases} 0 & NON-KIN \\ 1 & KIN \end{cases}. \quad (2)$$

Note, a \mathbb{P}_s consists of a pair of templates and, thus, the task is to determine whether the media of the templates provide evidence that the two persons are blood relatives; notice Eq. (2) is the template *matcher* defined in Eq. (1).

The data can be further split by the type of relationship l — L sets of pairs organized into L independent lists, meaning \mathbb{P}_s partitioned into l disjoint sets in \mathbb{P}_s^l (Table 3). Specifically, pair-types are brother-brother (BB), sister-sister (SS), or brother-sister (SIBS) of mixed-sex; father-daughter (FD), father-son (FS), mother-daughter (MD), or mother-son (MS); grandfather-granddaughter (GFGD), grandfather-grandson (GFGS), grandmother-granddaughter (GMGD), or grandmother-grandson (GMGS); four *great grandparent* types as well. Hence, $l \in L \rightarrow \{BB, SS, \dots, GMGD, GMGS\}$ with $L = 11$. Statistics for all relationship types are listed in Table 2, with the lists of *grandparent-grandchild* and *great grandparent* omitted from verification task due to insufficient sample counts (*i.e.*, $L = 7$).

As described, FIW-MM is organized as templates with many samples from various modalities (*i.e.*, still-face, face-tracks, audio, and transcripts (contextual)). Specifically, true IDs y are paired with a template of all media available for the respective subject. In contrast with conventional kinship recognition, where one image is compared to another, the 1:1 paradigm is template-based (*i.e.*, one template compared to another). Then, a template pair $\mathbb{P}_s^l = ((X_i, y_i), (X_j, y_j))$ is of different subjects (*i.e.*, X_i and X_j , where $i \neq j$).

Table 5: Identification results, with TA highlighted. Accuracy scores for different ranks are listed (*i.e.*, higher is better). Also, mAP scores are provided for each.

		Rank					mAP
		@1	@5	@10	@20	@50	
img	mean	0.29	0.43	0.54	0.64	0.78	0.13
	median	0.28	0.44	0.52	0.64	0.77	0.13
	max	0.11	0.19	0.28	0.34	0.52	0.06
	TA	0.31	0.43	0.52	0.63	0.74	0.14
img+video	mean	0.30	0.44	0.52	0.64	0.77	0.14
	median	0.28	0.44	0.50	0.63	0.76	0.14
	max	0.13	0.21	0.26	0.30	0.44	0.06
	TA	0.34	0.46	0.55	0.68	0.75	0.16
img+video+audio	mean	0.30	0.44	0.52	0.64	0.77	0.14
	median	0.28	0.44	0.50	0.63	0.76	0.14
	max	0.13	0.21	0.26	0.30	0.44	0.06
	TA	0.56	0.59	0.63	0.74	0.78	0.24

4.2.2 Metrics

Detection Error Trade-off (DET) curves, along with average verification accuracy, were used for kinship verification. As too were TAR scores at intervals of FAR values (Table 4).

DET curves show error rates for binary classification systems, plotting the false-negative rate (FNR) as a function of FAR. Type II error FNR contributes to the Type I error False-positive rate (FPR) revealing the *imposter* falsely accepted:

$$\text{FAR} = \text{FPR} = \frac{\text{FP}}{N^-} = \frac{\text{FP}}{\text{FP} + \text{TN}},$$

where the count of negatives is N^- . The geometric relationships of the metrics related to the score distributions and the choice in threshold show the trade-offs in error rates (*i.e.*, Type I versus Type II error):

$$\text{FNR} = \frac{\text{FN}}{N^+} = \frac{\text{FN}}{\text{FN} + \text{TP}}.$$

In summary, a variety of attempts are made for both *genuine* and *imposter* pairs, for which scores are saved. Then, by changing the threshold that converts the score to a decision, we are able to visualize the trade-offs between the different error types (*i.e.*, lower threshold means fewer rejections of *genuine* pairs, but more passing of *imposter* pairs). Thus, the performance of the system is highly dependent on a choice in threshold, which is the reason DET curves are often used in biometrics to observe these trade-offs in binary problems.

4.3 Search & retrieval (missing family member)

Kinship identification is organized as a 1:N search and retrieval task, with each subject having one-to-many media samples. Thus, we imitate template-based evaluation protocols [41]. Furthermore, the goal is to find relatives of search subjects (*i.e.*, *probes*) in a search pool (*i.e.*, *gallery*).

4.3.1 Data splits and settings

A gallery $G = \{g_i\}, (i = 1, \dots, N)$ is queried by a set of probes $P = \{p_j\}, (j = 1, \dots, M)$ for search and retrieval, where g_i is the i -th template in G and p_j is the template of the j -th query subject. As mentioned, a template consists of samples of various modalities. Given a template of MM, various schemes were applied to integrate the identity information from all media components of P .

4.3.2 Metrics

Scores of N missing children are calculated as

$$AP(l) = \frac{1}{P_L} \sum_{tp=1}^{P_L} \text{Prec}(tp) = \frac{1}{P_L} \sum_{tp=1}^{P_L} \frac{tp}{\text{rank}(tp)},$$

where average precision (AP) is a function of family $l \in L$ (*i.e.*, $|L| = P_L$) for a given true-positive rate (TPR). All AP scores are averaged to find the mean AP (*i.e.*, mAP):

$$mAP = \frac{1}{N} \sum_{l=1}^N AP(l).$$

Also, Cumulative Matching Characteristic (CMC) curves as a function of rank enable for analysis between different attempts [71], along with the accuracy at rank 1, 5, and 10.

Our choice in metrics is typical for judging ranking capabilities of classification (or identification) systems. Like the DET assesses the 1:1 case of verification, CMC measures the 1:m performance in ranking-based problems.

5 BENCHMARKS

5.1 Methodology

The problems of FIW-MM have various views— multi-source and multi-modal. The former varies in samples and in treating the different media-types independently until the matching function outputs scores (*i.e.*, late-fusion). The latter demands a method for early fusion (*e.g.*, feature-level) which should enhance performance by leveraging informative samples while ignoring noisy and less discriminative samples. We next describe the modality-specific features (*i.e.*, encoding different media types), and methods of fusion.

5.1.1 Visual features

Each visual media sample is represented as the encoding from Arcface CNN [64] (*i.e.*, ResNet-34). MS1M [72] was the train set, which contained ≈ 5.8 M faces for 85,000 subjects. Faces were detected with MTCNN [63] returning the five facial landmarks (*i.e.*, two eyes, nose, both corners of the mouth). Then, faces were cropped and aligned using a similarity transformation on the five points with references set by the eye locations. Once cropped the faces were resized to 96×112 . The RGB (*i.e.*, pixel values of [0, 255]) were center about 0 (*i.e.*, subtracting 127.5) and then standardized (*i.e.*, divided by 128). The images are then mapped to features by passing through CNN— all encodings were later L2 normalized [66]. During training, the batchsize was 200, and a SGD optimizer with a momentum 0.9, weight decay $5e-4$, and learning rate starting at 0.1 and decreasing $10 \times$ twice, both times when the error leveled. These settings was made based on the SOTA reports on Arcface— a popular choice for an off-the-shelf option for FR technology and applications.⁵

Both images and videos are processed as described, with the mapping from image-space to feature-space denoted by $\mathcal{F}(x) \in \mathbb{R}^d$, where the dimension $d = 512$ for ArcFace. Face tracks from video data are fused to a single encoding by average pooling the encodings of the same track. Put formally, a face track of M frames is represented as $\bar{z} = \frac{1}{M} \sum_x \mathcal{F}(x)$. This reduces the effect of noisy frames, and smooths out the final representation to weigh just as all other media samples.

5. Followed <https://github.com/deepinsight/insightface>.

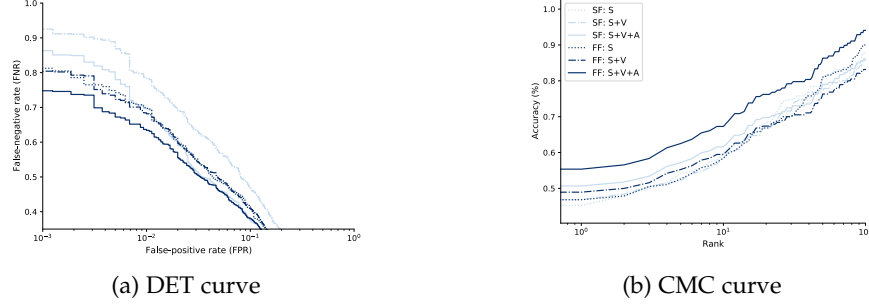


Figure 3: Results for score fusion (SF) and feature fusion (FF), or late and early fusion, respectively. Still-images S , video clips V , and audio segments A , with still-images and video $S + V$, and also still-images, audio, and video $S + V + A$. Clearly, both tasks benefit from early fusion: the DET curve (left) summarizes the verification task by plotting FNR versus FPR (*i.e.*, lower is better); search & retrieval shows a CMC curve (right)– accuracy across ranks (*i.e.*, higher is better).

5.1.2 Audio features

All speech segments were encoded with a SOTA deep learning architecture [67]. Specifically, we trained SqueezeNet [73] as a 34-layer ResNet [74] with an *angular prototypical loss* and optimized with Adam [75] to transform WAV-encoded audio files to a single encoding, *i.e.*, $f(x) = z \in \mathcal{R}^{512}$ per *Angular prototypical loss* [76] learns a metric alongside softmax to minimize within-class scatter (*i.e.*, penalty formed as the sum of euclidean distances from all samples of a subject in a mini-batch from the mean centroid of the respective mini-batch). Specifically, a support set S and a query Q are set in each mini-batch on a subject-by-subject basis, with Q made-up of a single utterance to compare with the centroid of S that consists of all other samples in the mini-batch for that class. *Angular prototypical* takes advantage of the perks of using centroid prototypes, while enhancing by following generalised end-to-end (GE2E) [77] usage of a cosine-based similarity metric. This is scale invariant, is more robust to feature variance, and facilitates stability in convergence during training [78].

5.1.3 Naive fusion

We demonstrate results from a variety of naive fusion techniques (*e.g.*, average pooling of features or voting of scores). To no surprise, the score-based fusion outperforms the naive feature-level fusion schemes. Specifically, the mean of all scores, both within a template and comparing templates (Table 4). The gain from each added modality is clear from just the naive score-fusion. Still, the naive fusion methods at the feature level are an ineffective way of combining knowledge. Provided media - media that varies in modality, quality and discriminative power - a simple, unweighted average across the items of a template does not exploit all information. To better fuse the template, we adapt a model to the template to better discriminate family members.

5.1.4 Feature fusion

Template adaptation (TA) [79] is a form of transfer learning that fuses labeled face encodings from a source domain with a template specific Support Vector Machines (SVMs) trained on the target domain. For kinship verification, *probe adaptation* settings are followed; for identification (*i.e.*, search & retrieval), we follow *gallery adaptation* settings. Regardless of which setting, the goal is to train a similarity function from a probe template P to either reference template Q (*i.e.*,

similarity $s(P, Q)$ for verification) or gallery G (*i.e.*, similarity $s(P, G)$ for identification) for *probe adaptation* and *gallery adaptation*, respectively. Thus, given a probe (*i.e.*, template), we train an SVM on top of its encoded media in x^+ as the positive samples and a set of negatives x^- : the main difference being that for verification (*i.e.*, *probe adaptation*) the negative set is formed by sampling a single sample from all other templates to use for P and Q , while for identification (*i.e.*, *gallery adaptation*) the negatives are of templates in $G = \{X_1, X_2, \dots, X_m\}$ besides the i^{th} template $X_i \neq X$. Either way, TA allows for early fusion of different media types while assuming many more negative samples (*i.e.*, $x^+ \ll x^-$). Furthermore, the variable number of positive samples, which is always much less than negative, and often only a few in itself, the SVM-based modeling mitigates issues of imbalance when comparing N_+ across the set of templates; particularly, cases with one or few samples are handled best in the kernel space defined by max-margins.

Finally, let $P(q)$ represent the evaluation of media encodings of template Q upon being trained on P , and vice versa for $Q(p)$ to leverage knowledge from both direction:

$$s(P, Q) = \frac{1}{2}P(q) + \frac{1}{2}Q(p). \quad (3)$$

The similarity score is the result of the templates fused.

The benefit of SVMs is in the kernel. Specifically, the linear, max-margin modeling scheme of a vanilla SVM has proven effective at separating a non-linear feature space between two classes; (*i.e.*, i and j , where $y_{ij} = \pm 1$ for the same (+) and different (−) classes). Thus, the implicit embedding function (*i.e.*, kernel) $K(x_i, x_j, y_{ij}) = \varphi(x_i, y_i)\varphi(x_j, y_j)$ projects the encoding pair to a non-linear space such that the SVM learns the best hyperplane $\mathbf{w}^T K(x_i, x_j, y_{ij}) + b = 0$ separating the two classes. This is done on training set by (1) maximizing the margin and (2) minimizing the loss-weights \mathbf{w} are learned, while bias terms b are set to 1 (*i.e.*, concatenated on \mathbf{w} as an added dimension). Also, $K(x_i, x_j, y_{ij}) = \exp \frac{\|x_i - x_j\|^2}{2\sigma^2}$ for $y_{ij} \in \{-, +\}$ as the respective class (*i.e.*, Gaussian RBF kernel [80] projects all encodings to a higher dimension). Then, the predicted class is inferred as $\hat{y} = \mathbf{w}^T \varphi(x_i)\varphi(x_j) + b$. We used *dlib*'s [81]– L2 regularized cosine-loss with class-weighted hinge-loss, *i.e.*,



Figure 4: Template of a true FS pair that was incorrectly classified using score fusion, but correct for TA (*i.e.*, feature fusion). Here only a single face is available for the father (left), while all instances of the son are at a young age (right).

$$\min_{\mathbf{w}} \frac{1}{2} \mathbf{w}^T \mathbf{w} + \lambda_+ \sum_{i=1}^{N_+} \max[0, 1 - y_i \mathbf{w}^T f(x_i)]^2 + \lambda_- \sum_{j=1}^{N_-} \max[0, 1 - y_j \mathbf{w}^T f(x_j)]^2. \quad (4)$$

Adapting this to the notion of a gallery, the protocols are set for *gallery adaptation*: train a similarity function $s(P, G)$ from a probe P to gallery G . A gallery of templates $G = \{X_1, X_2, \dots, X_m\}$ are used to train the SVM (*i.e.*, the scoring function $s(P, X_i)$). The difference between *probe adaptation* and *gallery adaptation* is in the negative sets. Along with the sample per subject trained against for *probe adaptation*, *global adaptation* samples all other templates in G as additional negatives. Again, $N_+ \ll N_-$. The class imbalance is handled via class-weighted hinge-loss in Eq 4, with $\lambda_+ = \lambda \frac{N_+ + N_-}{2N_+}$, $\lambda_- = \lambda \frac{N_+ + N_-}{2N_-}$, which are regularization constants inversely proportionate to class frequency. The constant λ trades-off between the regularization and loss, which we set to 10 as in previous work [79].

5.1.5 Implementation

The system was implemented in Python, with CNNs for both visual and audio from the PyTorch’s deep learning framework for each media encoders and SVM from LibSVM. The negative sample set was formed by randomly selecting a single instance from all other families. Hence, investigating and improving on the naive means for which we pool negative samples is a promising direction for future work. With that, N_+ and N_- is set case-by-case.

5.2 Results

System performance boosted with each added modality (Fig. 3, Table 4 and 5). Considering the benchmarks use conventional speech and FR technology, and our hypothesis that video and audio boosts discrimination, these notable improvements would likely continue to climb provided a more sophisticated or specific solution. It would be interesting to fuse earlier on, and train machinery jointly for audio-visual data. From this, more complex dynamics of facial appearance, along with the corresponding speech signal, could further our knowledge and give additional insights.

There was a trend in the type of samples that were corrected when comparing the score-based fusion to the feature-based (*i.e.*, TA). As shown in Figure 4, the challenge of recognizing kinship from samples of one or more member at a young age is mitigated. TA learns to better discriminate in these conventional failure cases. Additionally, some templates made up of multiple instances are often better than others when comparing. Hence, TA does not simply average

all instances equally, like for naive score-based fusion—fix cases with few samples are most discriminate (Fig. 5).

5.3 Discussion

The template-based protocol adds practical value by mimicking the more likely structure posed in operational settings, per NIST [41]. Besides, several other factors make it a more interesting formulation and therefore, a higher potential for researchers to show-off their creativity. For instance, opposed to using a single sample per subject (*i.e.*, one-shot learning), each now is represented in a set of media (*i.e.*, a template). The question now arise - how to best fuse knowledge and incorporate evidence from different modalities and how to best learn from all available MM data? Another consequence of using templates is that the random chance is increased from (1) the knowledge added to pool (or fuse) from the added modalities, and (2) the gallery size reduces from tens of thousands by nearly ten-fold. The latter is not an implication of lesser difficulty, but the byproduct of reducing bias in data [43]. That is, opposed to having one-to-many samples per subject, there is just one template. Mitigating certain sources of data imbalance (*i.e.*, whether there are thirty samples or just one) a system’s ability to recognize a particular pairing or group affects the metric evenly for all. In other words, a system may easily recognize a specific parent-child pair - regardless of the number of face samples and, consequently, the number of face pairs. Hence, the impact on the metric is proportional to the number of unique pairs, not sample pairs.

Furthermore, for verification, we measured the impact of the different results using the standard significant test. Specifically, we set the baseline image-only as the null hypothesis to compare to an alternative hypothesis set as the different results (*i.e.*, image-only, image and video, and audio-visual). Specifically, comparing baseline to null results in a p-value of 1.000 (*i.e.*, same results). Then, a limited improvement p-value=0.974 (*i.e.*, smaller is better) results when compared to the mean of image and videos (*i.e.*, videos add samples, but of the similar modality after averaging frames). Significant improvement in p-value=0.024 when comparing with the naive fusion of multimedia (*i.e.*, audio and visual), which goes to 0.000 for TA using multimedia. Thus, this further validates our claim that kinship recognition systems significantly better the decisions.

6 FUTURE WORK

FIW-MM pushes the bar for possibilities in automatic recognition of kinship in MM. An immediate next step for research involves the gathering experts of different domains, such as those in sequence-to-sequence modeling, whether video (*i.e.*, visual), audio (*i.e.*, speech), contextual (*e.g.*, conversations, parts-of-speech, *etc.*), or early-fusing pairs or groups. Let us next discuss a variety of ways that we foresee the data being beneficial and as a means to form synergy amongst different research communities, and beyond (*i.e.*, although FIW-MM is for non-commercial uses, the resource has high commercial potential and, thus, *proof of principle* experiments can motivate business moves).

We expect FIW-MM will bring experts of anthropology and genealogy-based together with researchers of MM and



Figure 5: A MS pair incorrectly classified with late fusion, but correct with early fusion (*i.e.*, TA). The young age of the son and with most faces of the mother occluded by sunglasses pose a challenge (*i.e.*, score fusion puts equal weight on all samples, where TA learns to better discriminate).

ML to help identify the hidden patterns connecting families in MM. For instance, we showed that by simply applying pre-trained models from the speech recognition domain allows for the audio signal to be incorporated for more discriminative power than with visual evidence alone. Surely, there is room to improve over the simple benchmark. Furthermore, high-level semantics (*i.e.*, attributes) like accents, commonly used phrases, and speaker demeanor, could boost the overall performance and also provide insights by interpretation. Similarly, studies on familial language components and inherited changes, or even deltas across the same generation (*i.e.*, commonalities and differences in the speech of siblings) can too be quite revealing. A similar potential exists for the video tracks, and more so with audio-visual data, both in model complexity and practical uses.

The family trees, abundance of data points, rich meta-data for individuals and relationships among MM data – FIW-MM could serve as a basis for group-based (*i.e.*, social) data mining. Additional data can enhance or target specific nature-based studies, traditional ML-based audio, visual, and audio-visual tasks, or even extend this dataset. Fusing audio-visual data is an ongoing, unanswered problem [16]. Note that FIW-MM in its entirety pose more problems than it solves: from the model training, to improvements made when dealing with missing or incomplete modalities, and even the data processing and data imbalance; from the underlying roots of the problem to the high-level semantics, similar to contemporary biometrics systems with audio-visual data, FIW-MM is an appropriate step considering the state in visual kinship recognition technology.

Another direction is fusion. We included early and late fusion by joining the different media as features and scores, respectively. Scores were fused by naively averaging– ignoring the signal type, and assuming all samples should carry the same weight. Fusion can incorporate more sophisticated techniques: cross-modality, selectively choosing the highest quality samples, or a modal-based decision trees. This concept, alone, is vastly in need of solutions– whether data fusion, where the input is clips of aligned audio-visual data; early-fusion, as we did via TA to fuse at the feature-level; or late-fusion, which we also included by naively averaging scores. Besides, meta-knowledge, like relationship types (*e.g.*, directional relationships that inherently exist), genders, age, and other attributes, could indicate final decisions. Hence, there are an abundance of fusion paradigms– none are trivial, yet most hold promise.

Besides, questions concerning bias– trends as a function of gender and ethnicity; properly securing family data, addressing areas of privacy and protection. Furthermore,

studies on differences between a diverse pool versus a search pool of mostly similar faces– whether it be a closer look at the effects of age for different relationship types, quantifying the similarity of specific features across different subgroups, and its effects on appearance (*i.e.*, visual data) and speech (*i.e.*, audio data).

Research topics to spawn off the proposed are vast; the specifics suggested here are limited by our perception. We expect scholars and experts of other domains to see paradigms not mentioned here: whether it be an improved variant of adapting templates and feature fusion (*e.g.*, [82]), deciding when to fuse, a new method of integration, along with the integration details, are all open research questions.

7 CONCLUSION

We extended *Families In the Wild* (FIW) image dataset for kinship recognition with multimedia (MM) data– 1-3 MM samples for 2-4 members from 200 (of 1,000) families we obtained, and then renamed *FIW in Multimedia* (FIW-MM), which is the first dataset to provide multimedia data for families in ML-related fields. In addition, new paradigms (*i.e.*, template-based protocols) are followed in both benchmarks (*i.e.*, kinship verification and search & retrieval of family members)– templates mimic a realistic setting, as followed in FR-related problems, but with this a first for kin-based recognition. Our labeling pipeline uses multi-modal evidence and a simple feedback schema to leverage the labeled data of FIW to propagate ground truth for the added modalities. Results improve with each added media type, with the top performance obtained with early fusion of features of multiple modalities. FIW-MM marks a major milestone for kin-based problems by welcoming experts of other data domains. In addition, FIW-MM supports a number of MM recognition tasks due to its rich metadata, template-based structure and multiple modalities.

REFERENCES

- [1] W. Liu, Y. Wen, Z. Yu, M. Li, B. Raj, and L. Song, “Sphereface: Deep hypersphere embedding for face recognition,” in *Conference on Computer Vision and Pattern Recognition (CVPR)*, 2017.
- [2] I. Masi, Y. Wu, T. Hassner, and P. Natarajan, “Deep face recognition: A survey,” in *2018 31st SIBGRAPI conference on graphics, patterns and images (SIBGRAPI)*. IEEE, 2018, pp. 471–478.
- [3] R. Fang, K. D. Tang, N. Snavely, and T. Chen, “Towards computational models of kinship verification,” in *International Conference on Image Processing (ICIP)*. IEEE, 2010.
- [4] J. P. Robinson, M. Shao, and Y. Fu, “To recognize families in the wild: A machine vision tutorial,” in *ACM on International Conference on Multimedia (MM)*, 2018.
- [5] X. Qin, X. Tan, and S. Chen, “Tri-subject kinship verification: Understanding the core of a family,” *CoRR arXiv:1501.02555*, 2015.
- [6] J. P. Robinson, M. Shao, and Y. Fu, “Visual kinship recognition: A decade in the making,” *CoRR arXiv:2006.16033*, 2020.
- [7] J. P. Robinson, Y. Yin, Z. Khan, M. Shao, S. Xia, M. Stopa, S. Timoner, M. A. Turk, R. Chellappa, and Y. Fu, “Recognizing families in the wild: The 4th edition,” in *Conference on Automatic Face and Gesture Recognition*, 2020.
- [8] A. Ephrat, I. Mosseri, O. Lang, T. Dekel, K. Wilson, A. Hassidim, W. T. Freeman, and M. Rubinstein, “Looking to listen at the cocktail party: A speaker-independent audio-visual model for speech separation,” *CoRR arXiv:1804.03619*, 2018.
- [9] A. Nagrani, J. S. Chung, and A. Zisserman, “Voxceleb: a large-scale speaker identification dataset,” *CoRR arXiv:1706.08612*, 2017.
- [10] J. S. Chung, A. Nagrani, and A. Zisserman, “Voxceleb2: Deep speaker recognition,” *CoRR arXiv:1806.05622*, 2018.

- [11] A. Nagrani, S. Albanie, and A. Zisserman, "Seeing voices and hearing faces: Cross-modal biometric matching," in *Conference on Computer Vision and Pattern Recognition (CVPR)*, 2018.
- [12] S. Albanie, A. Nagrani, A. Vedaldi, and A. Zisserman, "Emotion recognition in speech using cross-modal transfer in the wild," in *ACM on International Conference on Multimedia (MM)*, 2018.
- [13] M. Hao, W.-H. Cao, Z.-T. Liu, M. Wu, and P. Xiao, "Visual-audio emotion recognition based on multi-task and ensemble learning with multiple features," *Neurocomputing*, 2020.
- [14] O. Wiles, A. Koepke, and A. Zisserman, "X2face: A network for controlling face generation by using images, audio, and pose codes," in *European Conference on Computer Vision (ECCV)*, 2018.
- [15] —, "Self-supervised learning of a facial attribute embedding from video," in *British Machine Vision Conference (BMVC)*, 2018.
- [16] X. Song, H. Chen, Q. Wang, Y. Chen, M. Tian, and H. Tang, "A review of audio-visual fusion with machine learning," in *Journal of Physics: Conference Series*, vol. 1237. IOP Publishing, 2019.
- [17] S. Petridis, Y. Wang, Z. Li, and M. Pantic, "End-to-end audiovisual fusion with lstms," *CoRR arXiv:1709.04343*, 2017.
- [18] J. P. Robinson, M. Shao, Y. Wu, and Y. Fu, "Families in the wild (FIW): Large-scale kinship image database and benchmarks," in *ACM on International Conference on Multimedia (MM)*, 2016.
- [19] P. G. Hepper, "Long-term retention of kinship recognition established during infancy in the domestic dog," *Behavioural processes*, vol. 33, no. 1-2, pp. 3-14, 1994.
- [20] P. Poindron, A. Terrazas, M. Oca, N. Serafin, and H. Hernandez, "Sensory and physiological determinants of maternal behavior in the goat (*capra hircus*)," *Hormones and behavior*, 2007.
- [21] P. Poindron, F. Lévy, and M. Keller, "Maternal responsiveness and maternal selectivity in domestic sheep and goats: the two facets of maternal attachment," *Developmental Psychobiology: The Journal of the International Society for Developmental Psychobiology*, 2007.
- [22] S. Xia, M. Shao, and Y. Fu, "Kinship verification through transfer learning," in *International Joint Conferences on AI (IJCAI)*, 2011.
- [23] S. Xia, M. Shao, J. Luo, and Y. Fu, "Understanding kin relationships in a photo," *IEEE Trans. on Multimedia*, 2012.
- [24] V. Vijayan, K. W. Bowyer, P. J. Flynn, D. Huang, L. Chen, M. Hansen, O. Ocegueda, S. K. Shah, and I. A. Kakadiaris, "Twins 3D face recognition challenge," in *IEEE International Joint Conference on Biometrics (IJCB)*. IEEE, 2011, pp. 1-7.
- [25] X. Zhou, J. Hu, J. Lu, Y. Shang, and Y. Guan, "Kinship verification from facial images under uncontrolled conditions," in *Proceedings of the 19th ACM international conference on Multimedia*. ACM, 2011.
- [26] R. Fang, A. Gallagher, T. Chen, and A. Loui, "Kinship classification by modeling facial feature heredity," in *International Conference on Image Processing (ICIP)*. IEEE, 2013.
- [27] J. Lu, X. Zhou, Y.-P. Tan, Y. Shang, and J. Zhou, "Neighborhood repulsed metric learning for kinship verification," *IEEE Trans. on Pattern Analysis and Machine Intelligence (TPAMI)*, 2014.
- [28] L. Zhang, Q. Duan, D. Zhang, W. Jia, and X. Wang, "Advkin: Adversarial convolutional network for kinship verification," *IEEE Transactions on Cybernetics*, 2020.
- [29] W. Wang, S. You, S. Karaoglu, and T. Gevers, "Kinship identification through joint learning using kinship verification ensemble," *CoRR arXiv:2004.06382*, 2020.
- [30] L. Zhang, K. Ma, H. Nejati, L. Foo, T. Sim, and D. Guo, "A talking profile to distinguish identical twins," *Image and Vision Computing*, 2014.
- [31] Y. Sun, J. Li, Y. Wei, and H. Yan, "Video-based parent-child relationship prediction," in *2018 IEEE Visual Communications and Image Processing (VCIP)*. IEEE, 2018, pp. 1-4.
- [32] M. Georgopoulos, Y. Panagakis, and M. Pantic, "Investigating bias in deep face analysis: The kanface dataset and empirical study," *CoRR arXiv:2005.07302*, 2020.
- [33] X. Wu, E. Granger, T. H. Kinnunen, X. Feng, and A. Hadid, "Audio-visual kinship verification in the wild," *International Conference on Biometrics (ICB)*, 2019.
- [34] J. P. Robinson, M. Shao, Y. Wu, H. Liu, T. Gillis, and Y. Fu, "Visual kinship recognition of families in the wild," *IEEE Trans. on Pattern Analysis and Machine Intelligence*, 2018.
- [35] Y. Wen, K. Zhang, Z. Li, and Y. Qiao, "A discriminative feature learning approach for deep face recognition," in *European Conference on Computer Vision (ECCV)*. Springer, 2016.
- [36] S. Wang, J. P. Robinson, and Y. Fu, "Kinship verification on families in the wild with marginalized denoising metric learning," in *Conference on Automatic Face and Gesture Recognition*, 2017.
- [37] Y. Wu, Z. Ding, H. Liu, J. P. Robinson, and Y. Fu, "Kinship classification through latent adaptive subspace," in *Conference on Automatic Face and Gesture Recognition*. IEEE, 2018.
- [38] F. S. Ghatas and E. E. Hemayed, "Gankin: generating kin faces using disentangled gan," *SN Applied Sciences*, 2020.
- [39] P. Gao, S. Xia, J. P. Robinson, J. Zhang, C. Xia, M. Shao, and Y. Fu, "What will your child look like? DNA-Net: Age and gender aware kin face synthesizer," *CoRR arXiv:1911.07014*, 2019.
- [40] C. Kumar, R. Ryan, and M. Shao, "Adversary for social good: Protecting familial privacy through joint adversarial attacks," in *Conference on Artificial Intelligence (AAAI)*, 2020.
- [41] B. Maze, J. Adams, J. A. Duncan, N. Kalka, T. Miller, C. Otto, A. K. Jain, W. T. Niggel, J. Anderson, J. Cheney et al., "Iarpa janus benchmark-c: Face dataset and protocol," in *International Conference on Biometrics (ICB)*. IEEE, 2018.
- [42] J. P. Robinson, M. Shao, H. Zhao, Y. Wu, T. Gillis, and Y. Fu, "Recognizing families in the wild (RFIW)," in *RFIW Workshop in ACM MM*, 2017.
- [43] J. P. Robinson, G. Livitz, Y. Henon, C. Qin, Y. Fu, and S. Timoner, "Face recognition: Too bias, or not too bias?" in *Computer Vision and Pattern Recognition Workshop*. IEEE, 2020.
- [44] Y. Li, J. Zeng, J. Zhang, A. Dai, M. Kan, S. Shan, and X. Chen, "Kinnet: Fine-to-coarse deep metric learning for kinship verification," in *RFIW Workshop in ACM MM*, 2017.
- [45] Q. Duan and L. Zhang, "Advnet: Adversarial contrastive residual net for 1 million kinship recognition," in *RFIW Workshop in ACM MM*, 2017.
- [46] X. Qin, D. Liu, and D. Wang, "A literature survey on kinship verification through facial images," *Neurocomputing*, 2019.
- [47] J. Lu, J. Hu, X. Zhou, J. Zhou, M. Castrillón-Santana, J. Lorenzo-Navarro, L. Kou, Y. Shang, A. Bottino, and T. Figueiredo Vieira, "Kinship verification in the wild: The first kinship verification competition," in *IEEE International Joint Conference on Biometrics*, 2014.
- [48] J. Lu, J. Hu, V. E. Liong, X. Zhou, A. Bottino, I. Ul, T. Figueiredo Vieira, X. Qin, X. Tan, and S. Chen, "kinship verification in the wild evaluation," in *Conference on Automatic Face and Gesture Recognition*, 2015.
- [49] X. Wu, E. Boutellaa, X. Feng, and A. Hadid, "Kinship verification from faces: Methods, databases and challenges," in *Conference on Signal Processing, Communications and Computing*. IEEE, 2016.
- [50] O. M. Parkhi, A. Vedaldi, and A. Zisserman, "Deep face recognition," in *British Machine Vision Conference*, 2015.
- [51] Q. Cao, L. Shen, W. Xie, O. M. Parkhi, and A. Zisserman, "Vg-gface2: A dataset for recognising faces across pose and age," in *Conference on Automatic Face and Gesture Recognition*, 2018.
- [52] T. Afouras, J. S. Chung, and A. Zisserman, "The conversation: Deep audio-visual speech enhancement," *CoRR arXiv:1804.04121*, 2018.
- [53] J. S. Chung and A. Zisserman, "Lip reading in profile," in *British Machine Vision Conference (BMVC)*, 2017.
- [54] T. Afouras, J. S. Chung, and A. Zisserman, "Deep lip reading: a comparison of models and an online application," in *INTER-SPEECH*, 2018.
- [55] J. S. Chung and A. Zisserman, "Lip reading in the wild," in *Asian Conference on Computer Vision (ACCV)*, 2016.
- [56] J. S. Chung, A. Senior, O. Vinyals, and A. Zisserman, "Lip reading sentences in the wild," in *Conference on Computer Vision and Pattern Recognition (CVPR)*, 2017.
- [57] J. S. Chung, A. Jamaludin, and A. Zisserman, "You said that?" in *British Machine Vision Conference (BMVC)*, 2017.
- [58] O. Wiles, A. Sophia Koepke, and A. Zisserman, "X2face: A network for controlling face generation using images, audio, and pose codes," in *European Conference on Computer Vision (ECCV)*, 2018, pp. 670-686.
- [59] S. Albanie, A. Nagrani, A. Vedaldi, and A. Zisserman, "Emotion recognition in speech using cross-modal transfer in the wild," in *ACM on International Conference on Multimedia (MM)*, 2018.
- [60] I. U. Haq, K. Muhammad, T. Hussain, S. Kwon, M. Sodanil, S. W. Baik, and M. Y. Lee, "Movie scene segmentation using object detection and set theory," *International Journal of Distributed Sensor Networks*, vol. 15, no. 6, p. 1550147719845277, 2019.
- [61] T. Ahonen, A. Hadid, and M. Pietikainen, "Face description with local binary patterns: Application to face recognition," *IEEE Trans. on Pattern Analysis and Machine Intelligence (TPAMI)*, 2006.
- [62] E. Sánchez-Nielsen, F. Chávez-Gutiérrez, J. Lorenzo-Navarro, and M. Castrillón-Santana, "A multimedia system to produce and

deliver video fragments on demand on parliamentary websites,” *Multimedia Tools and Applications*, vol. 76, no. 5, 2017.

- [63] K. Zhang, Z. Zhang, Z. Li, and Y. Qiao, “Joint face detection and alignment using multitask cascaded convolutional networks,” *IEEE Signal Processing Letters*, vol. 23, no. 10, pp. 1499–1503, 2016.
- [64] J. Deng, J. Guo, N. Xue, and S. Zafeiriou, “Arcface: Additive angular margin loss for deep face recognition,” in *Conference on Computer Vision and Pattern Recognition (CVPR)*, 2019.
- [65] G. B. Huang, M. Ramesh, T. Berg, and E. Learned-Miller, “Labeled faces in the wild: A database for studying face recognition in unconstrained environments,” UMass, Amherst, Tech. Rep., 2007.
- [66] F. Wang, X. Xiang, J. Cheng, and A. L. Yuille, “Normface: L2 hypersphere embedding for face verification,” in *ACM on International Conference on Multimedia (MM)*, 2017, pp. 1041–1049.
- [67] J. S. Chung, J. Huh, S. Mun, M. Lee, H. S. Heo, S. Choe, C. Ham, S. Jung, B.-J. Lee, and I. Han, “In defence of metric learning for speaker recognition,” *CoRR arXiv:2003.11982*, 2020.
- [68] H. Zhu, M. Luo, R. Wang, A. Zheng, and R. He, “Deep audio-visual learning: A survey,” *CoRR arXiv:2001.04758*, 2020.
- [69] J. S. Chung and A. Zisserman, “Out of time: automated lip sync in the wild,” in *Workshop on Multi-view Lip-reading, ACCV*, 2016.
- [70] Y. Li, M. Murias, S. Major, G. Dawson, K. Dzirasa, L. Carin, and D. E. Carlson, “Targeting EEG/LFP synchrony with neural nets,” in *Advances in Neural Information Processing Systems (NIPS)*, 2017.
- [71] B. DeCann and A. Ross, “Relating ROC and CMC curves via the biometric menagerie,” in *IEEE International Conference on Biometrics: Theory, Applications and Systems (BTAS)*. IEEE, 2013.
- [72] Y. Guo, L. Zhang, Y. Hu, X. He, and J. Gao, “Ms-celeb-1m: A dataset and benchmark for large-scale face recognition,” in *European Conference on Computer Vision (ECCV)*. Springer, 2016.
- [73] F. N. Iandola, S. Han, M. W. Moskewicz, K. Ashraf, W. J. Dally, and K. Keutzer, “Squeezenet: Alexnet-level accuracy with 50x fewer parameters and <0.5mb model size,” *CoRR arXiv:1602.07360*, 2016.
- [74] K. He, X. Zhang, S. Ren, and J. Sun, “Deep residual learning for image recognition,” in *Conference on Computer Vision and Pattern Recognition (CVPR)*, 2016, pp. 770–778.
- [75] D. P. Kingma and J. Ba, “Adam: A method for stochastic optimization,” *CoRR arXiv:1412.6980*, 2014.
- [76] J. Snell, K. Swersky, and R. Zemel, “Prototypical networks for few-shot learning,” in *Advances in Neural Information Processing Systems (NIPS)*, 2017, pp. 4077–4087.
- [77] L. Wan, Q. Wang, A. Papir, and I. L. Moreno, “Generalized end-to-end loss for speaker verification,” in *International Conference on Acoustics, Speech and Signal Processing (ICASSP)*. IEEE, 2018.
- [78] J. Wang, F. Zhou, S. Wen, X. Liu, and Y. Lin, “Deep metric learning with angular loss,” in *IEEE International Conference on Computer Vision (ICCV)*, 2017, pp. 2593–2601.
- [79] C. Whitelam, E. Tabor, A. Blanton, B. Maze, J. Adams, T. Miller, N. Kalka, A. K. Jain, J. A. Duncan, K. Allen et al., “Iarpa janus benchmark-b face dataset,” in *IEEE Conference on Computer Vision and Pattern Recognition (CVPR) Workshop*, 2017.
- [80] B. Schölkopf, A. J. Smola, F. Bach et al., *Learning with kernels: support vector machines, regularization, optimization, and beyond*. MIT, 2002.
- [81] D. E. King, “Dlib-ML: A machine learning toolkit,” *The Journal of Machine Learning Research*, vol. 10, pp. 1755–1758, 2009.
- [82] L. Xiong, J. Karlekar, J. Zhao, Y. Cheng, Y. Xu, J. Feng, S. Pranata, and S. Shen, “A good practice towards top performance of face recognition: Transferred deep feature fusion,” *CoRR arXiv:1704.00438*, 2017.

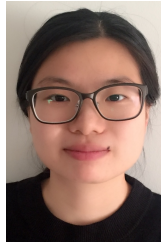


Joseph P. Robinson B.S. in electrical & computer engineering ('14) and Ph.D. in computer engineering ('20) at Northeastern University, where he also works as part-time faculty: designed and taught undergraduate course in Data Analytics ('19-'20 *Best Teacher*). Research is in applied machine vision, with emphasis on faces, deep learning, MM, and big data. Led on TRECVID debut (MED'15, 3rd place). Built many image and video datasets—most notably FIW. Organized & hosted several workshops

and challenges (e.g., NECV17, RFIW@ACMMM17, RFIW@FG18-20, AMFG@CVPR18, FacesMM @ICME18-19), tutorials (ACM-MM18, CVPR19, FG19), PC member (e.g., CVPR, FG, MIRP, MMEDIA, AAAI, ICCV, etc.), reviewer (e.g., IEEE TBioCAS, TIP, TPAMI, etc.), and Pres. of IEEE@NEU and Rel. Officer of IEEE SAC R1 Region. Completed NSF REUs ('10 & '11); co-op at Analogic Corp. ('12) BBN Tech. ('13); intern at MIT LL ('14), STR ('16-'17), Snap Inc. ('18), ISMConnect ('19).



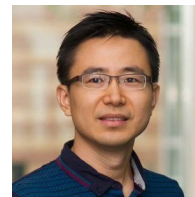
Zaid Khan Received a B.S. in Computer engineering ('18) and is currently a Ph.D. student in Computer Engineering ('25) at Northeastern University under Dr. Yun Fu. Zaid served as the website and technical chair of RFIW 2020 held in conjunction with IEEE Conference on Facial and Gesture Recognition. His research interests lie in computer vision, with a focus on faces.



served as organizing chair of RFIW Workshop Challenge @ FG'20, conference PC (e.g., AAAI & FG), and journal reviewer (e.g., IEEE Trans. on TIP & TNNLS). She interned at Zillow Group (2020).



Ming Shao Received the B.E. degree in computer science, the B.S. degree in applied mathematics, and the M.E. degree in computer science from Beihang University, Beijing, China, in 2006, 2007, and 2010, respectively. He received the Ph.D. degree in computer engineering from Northeastern University, Boston MA, 2016. He is a tenure-track Assistant Professor affiliated with College of Engineering at the University of Massachusetts Dartmouth since 2016 Fall. His current research interests include sparse modeling, low-rank matrix analysis, deep learning, and applied machine learning on social media analytics. He was the recipient of the Presidential Fellowship of State University of New York at Buffalo from 2010 to 2012, and the best paper award winner/candidate of IEEE ICDM 2011 Workshop on Large Scale Visual Analytics, and ICME 2014. He has served as the reviewers for many IEEE Transactions journals including TPAMI, TKDE, TNNLS, TIP, and TMM. He has also served on the program committee for the conferences including AAAI, IJCAI, and FG. He is the Associate Editor of SPIE Journal of Electronic Imaging, and IEEE Computational Intelligence Magazine. He is a member of IEEE.



Yun Fu (S'07-M'08-SM'11-F'19) received the B.Eng. degree in information engineering and the M.Eng. degree in pattern recognition and intelligence systems from Xi'an Jiaotong University, China, respectively, and the M.S. degree in statistics and the Ph.D. degree in electrical and computer engineering from the University of Illinois at Urbana-Champaign, respectively. He is an interdisciplinary faculty member affiliated with College of Engineering and the College of Computer and Information Science at Northeastern University since 2012. His research interests are Machine Learning, Computational Intelligence, Big Data Mining, Computer Vision, Pattern Recognition, and Cyber-Physical Systems. He has extensive publications in leading journals, books/book chapters and international conferences/workshops. He serves as associate editor, chairs, PC member and reviewer of many top journals and international conferences/workshops. He received seven Prestigious Young Investigator Awards from NAE, ONR, ARO, IEEE, INNS, UIUC, Grainger Foundation; eleven Best Paper Awards from IEEE, ACM, IAPR, SPIE, SIAM; many major Industrial Research Awards from Google, Samsung, Amazon, Konica Minolta, JP Morgan, Zebra, Adobe, and Mathworks, etc. He is currently an Associate Editor of the IEEE Transactions on Neural Networks and Learning Systems. He is fellow of IEEE, IAPR, OSA and SPIE, a Lifetime Distinguished Member of ACM, Lifetime Member of AAAI, and Institute of Mathematical Statistics, member of Global Young Academy, INNS and Beckman Graduate Fellow during 2007-2008.